NEAR IR-AC COUPLED CCD DETECTOR ARRAY

George Domingo, Michael D. Jack, Joseph Y.M. Lee, Vincent T. Bly*

ABSTRACT

An Intrinsic Silicon Detector Array has been developed to operate in an environment of high illumination and low contrast. This device is an experimental 16 x 16 detector array to detect small modulation changes on a constant Near IR radiation generated by a GaAs or GaAlAs laser source. The array is a high resistance silicon backside illuminated structure to increase the collection area and thinned to create the electric fields required to collect all photoelectrons generated in the substrate.

The signal processing is performed on low resistance epitaxial region. The input is an ac coupled gate modulated structure needed to detect the small signal superimposed on a large photocurrent. Two level of Multiplexers and an on-chip output amplifier generate a voltage proportional to the change of IR.

The design, analysis, and operation of the array are discussed.

INTRODUCTION

The need for detectors capable of responding in the near IR spectral region has led to an increased interest in intrinsic silicon (ρ > 1000 ohms-cm) charge transfer devices. Only recently attempts have been made to increase the complexity of the arrays by increasing the number of detectors on the focal plane and by including signal processing capabilities in an epitaxial layer. One larger array of 160 detectors with 20 read out lines each addressing 8 detectors was fabricated at Hughes. This array[1] was a backside illuminated array and the detectors, of varying sizes, were defined by fully depleted junctions. A responsivity of 0.6 amps/watt with good uniformity (better than 10%) and minimal crosstalk (less than 4%) was obtained in the smaller center detectors (41 x 41 square microns).

The array reported here is a 16 x 16 test array, for front or backside illumination, with a unit cell of 100 x 100 square microns. The input is an ac coupled structure fabricated on a low resistivity epitaxial layer grown on an high resistivity substrate. Two level multiplexing read all the detectors in the focal plane through one output amplifier.

IR SYSTEM

The AC coupled visible imager described here will be used in a prototype Thermo-Optical FLIR system being developed at the Night Vision and Electro-Optics Laboratory.[2] The Thermo-Optical FLIR is similar, in principle, to the Absorption Edge Image Tube developed by Hilsum[3] in that the detecting phenomena is the thermal change in complex index of refraction of a semiconductor near its fundamental absorption edge. Hilsum's original system, which was direct view, was limited in sensitivity by the contrast discrimination of the observer. It was limited in temporal and spatial response by the relatively thick (> 1 μm) transducer (high heat capacity per unit area and substantial lateral heat transport). The Thermo-Optical FLIR differs by using a much thinner transducer (1000Å to 2000Å), and by chopping the infrared input and amplifying only the time varying portion of the transducer output (see Figure 1). In this way a significant improvement in resolution is achieved and the thermal sensitivity is improved to the photon shot noise limit of the reading beam. Analysis indicates[2] that a system using a stabilized LED laser, the improved transducer, and the NEAR IR-CCD array described here, can provide performance at least four times better than the best pyroelectric vidicons. Experimental tests, using a single visible - Near IR detector, have already demonstrated sensitivities below 1^{o} ΔT using a T/1.6 objective.

DESIGN CONSIDERATIONS

Calculations at NVEOL show that the illumination on the array from the laser is 4.3×10^{15} photons/cm^2-sec and the signal is 10^{-3} to 10^{-5} times the dc intensity. This small modulation on a rather large signal makes it necessary to design a dc suppressed array to assure sufficient dynamic range. Table I lists the desired performance parameters and Table II the calculated values of the photocurrent and background noise. A responsivity of 0.35 amps/watt and D* of 3.3×10^{10} cm$\sqrt{\text{Hz}}$/Watts can be obtained with a 100 x 100 square micron detector and a 50% quantum efficiency.

*G. Domingo, Hughes Aircraft Tactical Systems Division, Culver City, California; M.D. Jack and J.Y.M. Lee, Hughes Aircraft Company, Carlsbad Research Center, Carlsbad, California; V.T. Bly, Night Vision and Electro-Optical Laboratories, Fort Belvoir, Virginia.

Figure 2 shows the overall structure of the array. The radiation received by the detector generates a current that flows through the bias resistance and develops a voltage at the modulation gate. The current to the CCD is applied through a diffusion and the fat zero current, modulated by the modulation gate, is integrated in the storage bucket. At a frame rate of 30 or 60 Hz the transfer gate is turned on and the integrated charge, which is proportional to the signal, is transferred to a CCD multiplexer. Two columns of 16 detectors each transfer to the same multiplexer. Eight multiplexers transfer to the fast multiplexer and the signal is removed through an output amplifier. The sharing of one multiplexer by two columns of detectors saves valuable area and allows the gates to be larger thus increasing the dynamic range of the array.

a) Detector Thickness

One of the critical design considerations is the optimum detector thickness to obtain the highest responsivity with the lowest detector crosstalk and minimum optical saturation of the electronics. If the detector thickness is too large, very large voltages need to be applied across the detector in order to deplete the junction and thus assure that all the free charges generated by the photons are collected. If the depletion is not complete, the free photo charges can either recombine, decreasing the quantum efficiency, or they can migrate to surrounding detectors increasing the crosstalk. Figure 3 shows the relative photon intensity at different depth layers of the intrinsic silicon for several wavelengths. For the desired wavelength of 0.86 microns about 90% of the radiation has been absorbed in the first 50 microns and 99.9% of the radiation is absorbed in a depth of 100 microns. In order to maximize responsivity and decrease crosstalk it is desirable to have the majority of the photons absorbed in the depletion region. The photon generated electron-hole pairs are then separated by the electric field and the appropriate carrier is collected by the detector. Figure 3 also shows the depletion depth as a function of applied voltage and substrate resistivity. The figure shows that 50 micrometers can be fully depleted with a voltage of 20 volts if the substrate resistance is higher than 6 kΩ-cm.

Another consideration is the optical saturation of the electronics due to photons absorbed in the epitaxial region itself. The storage or integration gate is constructed on a six micrometer epitaxial layer. This epi layer will absorb 1.5% of the photons if the detector is backside illuminated. The charge generated under the storage gate due to photon absorption is 1.3×10^6 electrons, and the total charge capacity of the storage gate is 2.8×10^6 electrons. Under these conditions, half of the storage gate is full with photocharges. Several ways to circumvent this problem have been considered.

1. Increase the thickness of the wafer from 50 to 100 microns. Under these conditions about 0.1% of the radiation will be absorbed in the epitaxial layer. The substrate will not be fully depleted but in the present system, where a large, almost uniform radiation illuminates the back surface, full depletion may not be needed since the largest charge gradient will direct the carriers towards the collecting nodes.

2. Lower wavelength source. If the wavelength of the radiation is decreased from 0.86 to 0.8 microns, the absorption in the epitaxial layer decreases to about 0.3% of the radiation striking the back surface.

3. Front side illumination. All the arrays are provided with a light shield which protects the electronics. The detector active area is decreased from 100 x 100 microns to 57 x 62 microns.

b) Noise Considerations

The AC equivalent circuit of the input structure is shown in Figure 4. The transfer function A_i is defined as

$$A_i = \frac{i_{ccd}}{i_i} = \frac{-g_m (e_2 - e_3)}{i_i} \cdot i_3$$

Solving the nodal equations of the network with the assumptions $G_B > G_D + s(C_1 + C_c)$, $C_c > C_T + C_R$, $G_{FZ} < g_m$, $G_R < sC$, and $g_m > sC_T$, where G_B is the bias conductance, G_D the detector conductance, C_1 the input capacitance, C_c the coupling capacitance, C_T the modulation capacitance, C_R the reset capacitance, G_m the transconductance, and G_{FZ} the fat zero resistance, the transfer functions can be found to be approximately, $A_1 = g_m/G_B$, $A_2 = g_m/sC_c$, and $A_3 = g_m/G_{FZ}$.

More important for optimizing the performance of the array is the relative transfer functions $A_2/A_1 = G_B/sC_c$, and $A_3/A_1 = G_B/G_{FZ}$. These relative transfer functions indicate how the background noise is boosted over other noise sources. To optimize the performance of the array, the bias resistance must be as large as possible. Since the staring system operates at low frame rates, the effect of the coupling capacitance is quite important and a very high bias resistance is imperative.

Other transfer functions included in the calculations are the sampling function G_1, the reset transfer function G_2, the gain of the multiplexer $(1/f_cC_o)$ and the gain of the output amplifier G_o. In addition, the

noises that appear in the array ahead of the first CCD multiplexer are folded so that the output noise due to any of the noise sources in the input is given by

$$S_{gi} = G_o G_3 G_2 \sum_{\infty}^{\infty} G_1 A_i (f + nf_c)$$

The exact nodal equations were written in a computer program with the proper transfer functions. The noise was also integrated at the storage bucket in order to calculate the dynamic range of the array.

Figure 5 shows the input referred noise sources calculated using a bias resistance of 4×10^8 ohms and a high resistance value of 4×10^9 ohms. The effect of the coupling capacitance is quite obvious. At the lowest frequencies the noises are boosted over the background noise and its effect diminishes with increasing signal frequency.

A more careful analysis was performed to optimize the array. Figure 6 shows the D* and the dynamic range as a function of bias resistance and background. It shows that considerable improvement can be obtained both by decreasing the background and increasing the bias resistance. An additional advantage of decreasing the background flux is that a smaller bias voltage is required since the photocurrent is also smaller. A bias resistance of $2 \times 10^9\ \Omega$ was chosen as a baseline approach.

c) Leakage Currents

The leakage currents in a staring array with low frame rates must be kept small and uniform so that variations of leakage currents from cell to cell are not confused with the optical signal. A uniform leakage current in all 256 detectors should not affect the operation of the array.

The minimum voltage that must be detected in the modulation gate is 152 μvolts which requires the leakage current to be smaller than 10^8 amps/cm^2. Assuming that variations from cell to cell can be kept below 5%, the leakage currents must be controlled below 2×10^{-7} amps/cm^2.

DEVICE OPERATION

Figure 7 shows in detail how two detector columns transfer the integrated photocharges into one single CCD multiplexer and figure 8 shows the pulse sequence required to operate the array. The transfer pulse ϕ_{tr} transfers the charges under ϕ_1, for odd rows and ϕ_3 for even rows. ϕ_3 remains ON while ϕ_1 and ϕ_2 are pulsed so as to move the charge from ϕ_1 to ϕ_3. At this time all the signals are located under ϕ_3. The vertical CCD is now clocked normally for three periods, transferring the charges to the fast multiplexer at the end of the second and third periods. An extra period is needed to move the charges the extra bits at the end of the CCD.

The frame rate is 30 or 60 Hz. For a 60 Hz frame rate the vertical multiplexer is run at a fundamental frequency of 920 Hz with a burst frequency of 15840 Hz. The horizontal multiplexer is run continuously at 63.36 KHz.

EXPERIMENTAL RESULTS

As pointed out earlier one of the critical parameters is the bias resistance which must be sufficiently large to obtain the voltage gain required to boost the signal over the array noises. Test resistors were fabricated on 2 inch wafers and evaluated before processing the full arrays. The median is $2.3 \times 10^8\ \Omega$-cm^2, which corresponds to bias resistors in the array of $1.4 \times 10^9\ \Omega$, and a sigma of $2 \times 10^7\ \Omega$. 34 elements of the 168 test resistors have values larger or smaller than two sigma, but if the first elements in the perimeter of the wafer are removed, the number of elements 2 sigma away from the mean are decreased from 34 down to 13. The uniformity of the resistors on a die (5 x 5 mm) is considerably better, less than $1.5 \times 10^6\ \Omega$-cm^2 or less than 1% deviation.

Spot scans of test detectors on die thinned to 50 μm have been performed. Figure 9 shows the spot scans of four detectors under several applied biases. These detectors are smaller than the detectors on the main array, their dimensions decreasing from 60 x 60 to 30 x 30 micrometers. These test detectors had no CCD readout and were measured using a transimpedance amplifier. As the detector bias increases the crosstalk between detector decreases from 8 to 2 percent, and the responsivity increases by about 80%. Responsivities as high as 0.6 amps/watt have been measured.

CONCLUSIONS

The initial tests have shown successful operation of all the components of the Near IR detector array. The processing of complex input structures on an EPI-MOS process has been shown to yield operational electronics and detectors with high responsivity and negligible crosstalk.

Experiments are now being performed and additional data will be reported during the conference.

The authors would like to thank M.Y. Pines, D.H. Alexander and Ron Finnila for their support and contributions to the design and fabrication of the array.

REFERENCES

1. A Near IR PIN/CCD Detector Array, G.H. Hershman et al. Technology and Applications of Charge Transfer Devices Conference, San Diego, California, October 1978.
2. Advanced FLIR Concepts, V.T. Bly. Meeting of the IRIS Specialty group on Infrared Imaging, Ann Arbor, Michigan, February, 1977.
3. The Theory of Thermal Imaging and its Application to the Absorption Edge Image Tube, C. Hilsum and W.R. Harding. Infrared Physics, Vol. I, 1961.

TABLE I. DESIRED PERFORMANCE

Q_B	Photon Flux	4.3×10^{15} photons/cm^2-sec
A_d	Area detectors	100 x 100 micrometers
S_{max}	Signal (max)	4.3×10^{12} photons/cm^2-sec
S_{min}	Signal (min)	4.3×10^{10} photons/cm^2-sec
f	Frame Rate	30 Hz
η	Quantum efficiency	0.5
$(S/N)_{min}$	minimum S/N	2.25
λ	wavelength	0.86 micrometers

TABLE II. CALCULATED PARAMETERS

Background Current	$I_B = \eta A_d Q_B q$	3.55×10^{-8} amps
Background Shot Noise	$I_{BN} = \sqrt{2 I_B q}$	1.07×10^{-13} amps/$\sqrt{Hz}$
Responsivity	$R = 0.805 \eta \lambda$	0.35 amp/watt
D* Blip	$D^*_{BLIP} = R\sqrt{A_d/I_{BN}}$	3.32×10^{10} cm$\sqrt{Hz}$/watt
Minimum Detectable Signal	$I_{SM} = I_{BN}(S/N)_{min} \cdot \sqrt{5}$	5.38×10^{-13} amps

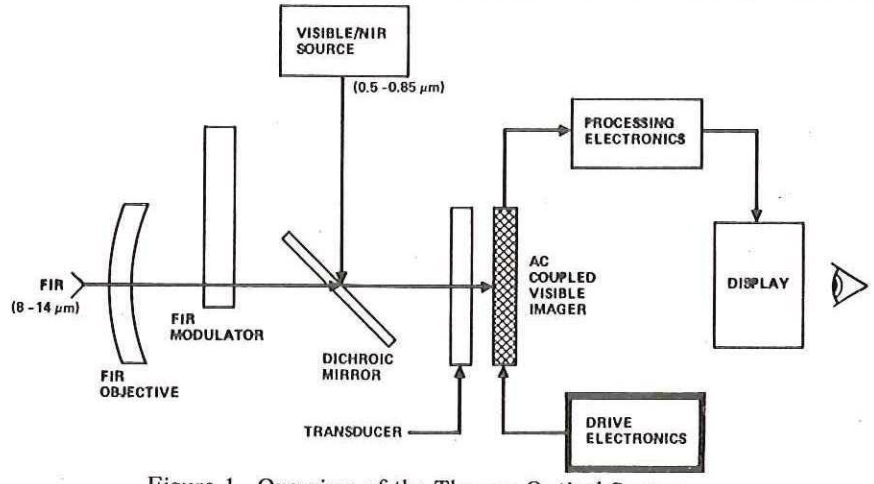

Figure 1. Overview of the Thermo-Optical System.

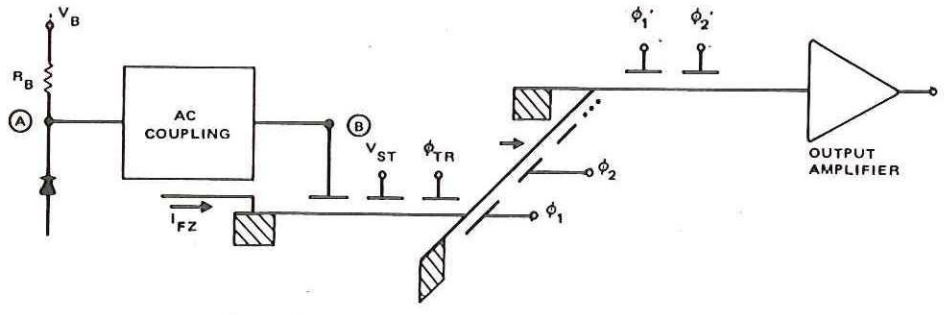

Figure 2. Input structure of near IR Imager.

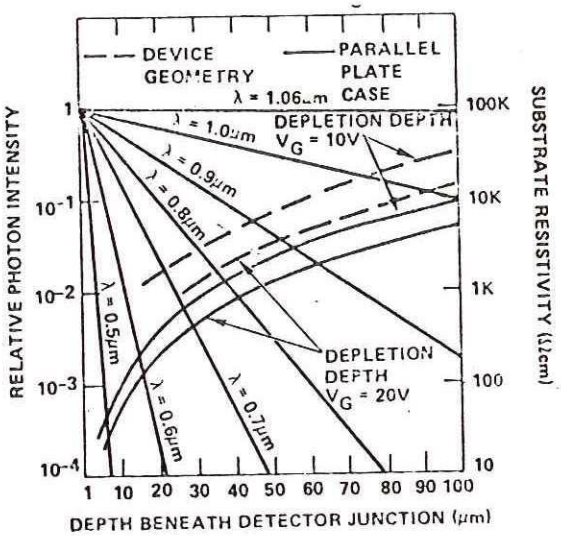

Figure 3. Decay at relative photon intensity for several wavelengths as a function of penetration depth into a silicon detector and depletion depth for voltages of 10 and 20 V as a function of substrate resistivity.

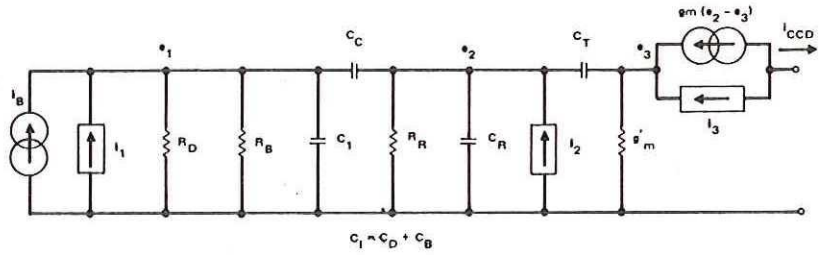

Figure 4. Equivalent model of the input structure.

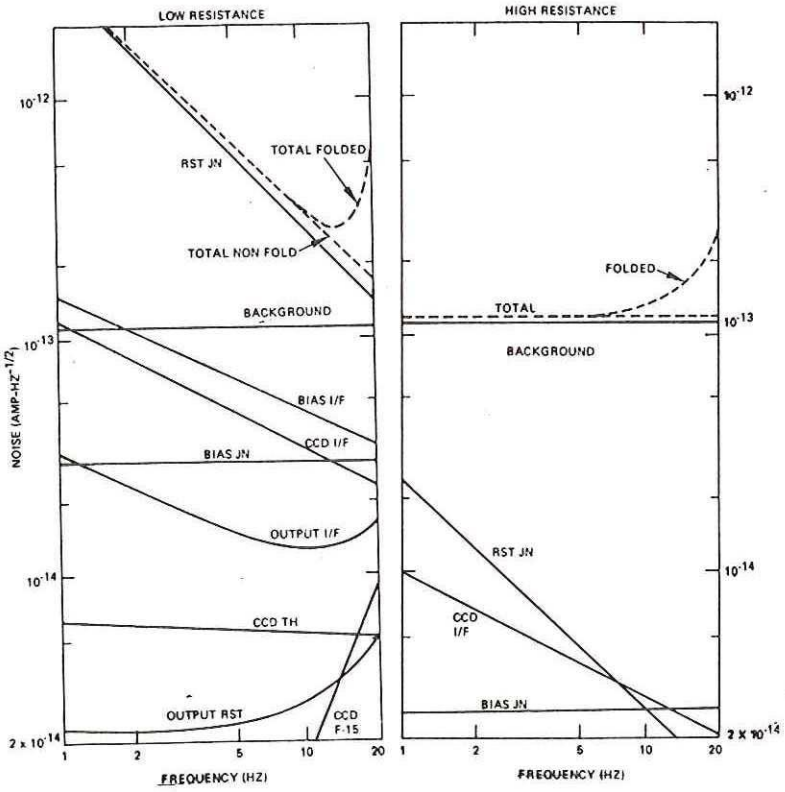

Figure 5. Noise components versus frequency for low and high bias resistance cases.

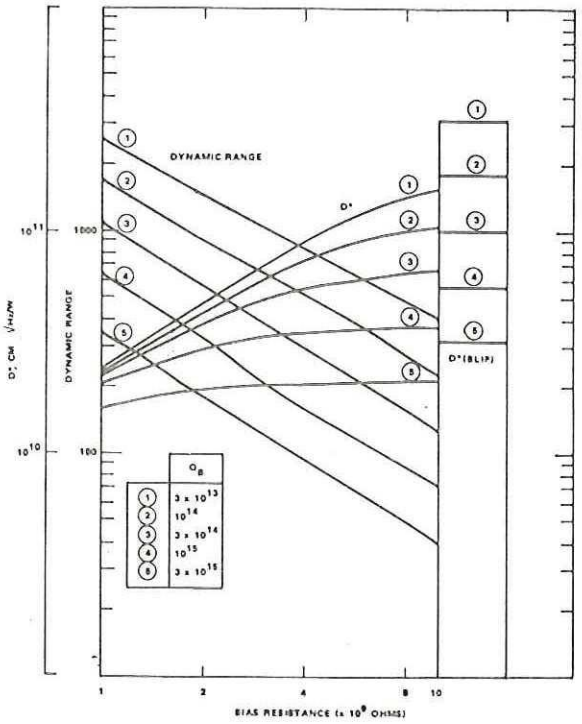

Figure 6. D* and dynamic range versus bias resistance as a function of background photo flux.

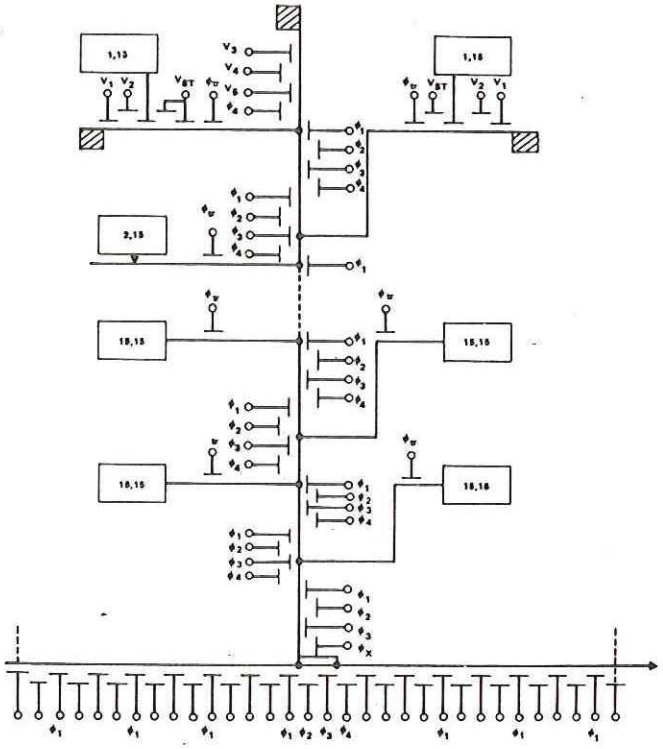

Figure 7. Detailed multiplexer circuit diagram.

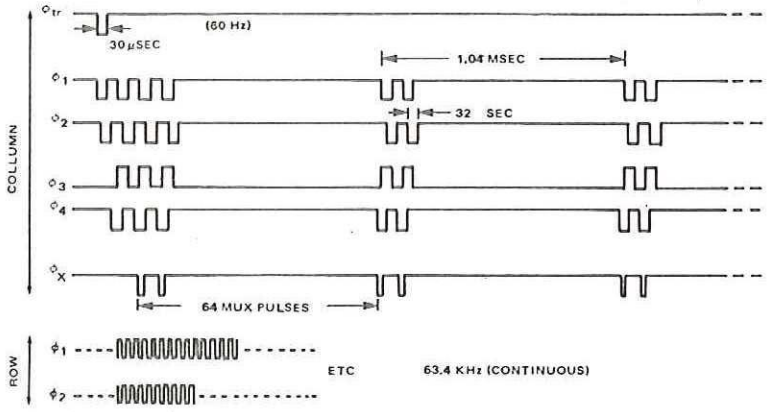

Figure 8. Pulses required to operate the AC coupled array.

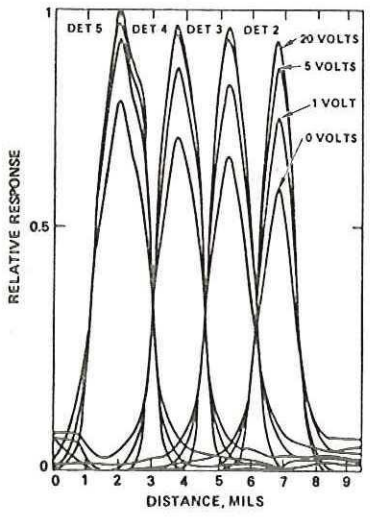

Figure 9. Relative detector response as a function of bias and spot position.